Published in final edited form as:

Oncogene. 2016 March 3; 35(9): 1122–1133. doi:10.1038/onc.2015.166.

LASP-1 – A nuclear hub for the UHRF1-DNMT1-G9a-Snail1 complex

Nichole Duvall-Noelle[1,*], **Ayub Karwandyar**[1,*], **Ann Richmond**[1,2], and **Dayanidhi Raman**[1,#,*]

[1]Department of Cancer Biology, Vanderbilt University, School of Medicine, Nashville, Tennessee, United States of America

[2]Tennessee Valley Healthcare System, Department of Veterans Affairs, Nashville, Tennessee, United States of America

Abstract

Nuclear LASP-1 has a direct correlation with overall survival of breast cancer patients. In this study, immunohistochemical analysis of a human breast TMA showed that LASP-1 is absent in normal human breast epithelium but the expression increases with malignancy and is highly nuclear in aggressive breast cancer. We investigated whether the chemokines and growth factors present in the tumor microenvironment could trigger nuclear translocation of LASP-1.Treatment of human breast cancer cells with CXCL12, EGF and Heregulin and HMEC-CXCR2 cells with CXCL8 facilitated nuclear shuttling of LASP-1. Data from the biochemical analysis of the nuclear and cytosolic fractions further confirmed the nuclear translocation of LASP-1 upon chemokine and growth factor treatment. CXCL12-dependent nuclear import of LASP-1 could be blocked by CXCR4 antagonist, AMD-3100. Knock down of LASP-1 resulted in alterations in gene expression leading to an increased level of cell junction and extracellular matrix proteins and an altered cytokine secretory profile. Three dimensional cultures of human breast cancer cells on Matrigel revealed an altered colony growth, morphology and arborization pattern in LASP-1 knock down cells. Functional analysis of the LASP-1 knock down cells revealed increased adhesion to collagen IV and decreased invasion through the Matrigel. Proteomics analysis of immunoprecipitates of LASP-1 and subsequent validation approaches revealed that LASP-1associated with the epigenetic machinery especially UHRF1, DNMT1, G9a and the transcription factor Snail1. Interestingly, LASP-1 associated with UHRF1, G9a, Snail1 and di- and tri-methylated histoneH3 in a CXCL12-dependent manner based on immunoprecipitation and proximity ligation assays. LASP-1 also

[#]Corresponding author: Dayanidhi Raman, B.V.Sc., Ph. D., Department of Cancer Biology, 436 Preston Research Building, 23rd Ave South @Pierce, Vanderbilt University Medical Center, Nashville, TN 37232, Tel.: 615-936-3332, Fax: 615-936-4687, ; Email: dayanidhi.raman@vanderbilt.edu

[*]Contributed equally

Supplementary information accompanies the paper on the Oncogene website – http://www.nature.com/onc

Author contributions

N.D-N: Acquisition and analysis of the data.

A.K.: Acquisition and analysis of the data.

A.R.: Interpretation of the data and manuscript preparation.

D.R.: Conception, design, execution, acquisition, analysis of the data and manuscript preparation.

Conflict of interest

The authors declare no conflict of interest.

directly bound to Snail1 which may stabilize Snail1. Thus, nuclear LASP-1 appears to functionally serve as a hub for the epigenetic machinery.

Keywords

Nuclear LASP-1; CXCL12; CXCR4; UHRF1; G9a; Snail1; Breast cancer

Introduction

LASP-1 (LIM and SH3 protein-1) is a scaffold protein that mediates cell migration, proliferation and survival in several human breast cancer cell lines ([1]). Silencing of LASP-1 in breast cancer cells inhibits cell migration and proliferation by 40% ([2, 3]). LASP-1 is organized into modular LIM, NR and SH3 domains and these domains interact with a variety of proteins. Previously, we discovered that LASP-1 directly binds to chemokine receptors CXCR1, CXCR2, CXCR3 and CXCR4 through its LIM domain ([4]) that are involved in directed migration of tumor and stromal cells ([5, 6]). This directional migration and local invasion facilitates the metastasis of breast cancer cells. Through its direct binding to the chemokine receptors, LASP-1 could be involved in modulating the signaling pathways evoked by these chemokine receptors and thus possibly provides a key potential target for interrupting the roles of CXCR2 ([4, 7–9]), CXCR4 ([10–14]) and CXCR3 ([15–17]) in primary and metastatic breast cancer.

A previous study showed that an elevated expression of LASP-1 in breast epithelial cells correlated with increased malignancy, tumor grade and lymph node status ([18]). This may suggest a role for LASP-1 in breast cancer progression and metastasis. Interestingly, nuclear LASP-1 (nLASP-1) is evident in 31% of LASP1-positive invasive breast cancer samples. Importantly, the nLASP-1 status and the 10-year survival rate are inversely correlated ([19]). Unraveling the mechanism by which nLASP-1 is linked to poor patient outcome may provide new key targets for treatment of subsets of breast cancer.

The tumor microenvironment is enriched with chemokines and growth factors. We tested whether the chemokines and growth factors present in the tumor microenvironment would potentially trigger the nuclear translocation of LASP-1. A role in chromatin remodeling for nLASP-1 has been suggested in human breast cancer, but at this time remain uncharacterized. Our data demonstrate for the first time that upon stimulation of human breast cancer cells with the chemokines CXCL12, CXCL8, and the growth factors epidermal growth factor (EGF) and heregulin (HRG) resulted in a shuttling of LASP-1 to the nucleus. By employing a variety of approaches, we discovered that LASP-1 associates with several novel proteins involved in epigenetic regulation of gene expression ([20, 21]). Moreover, we report here that LASP-1 directly binds to Snail1 and nLASP-1 may serve as a hub for several proteins involved in epigenetic regulation of gene expression. Our data uncover a novel role for nLASP-1.

Results

Expression of LASP-1 in normal and cancerous breast

To examine the subcellular status of the LASP-1 *in vivo* in normal human breast and cancerous breast tissue, de-identified, commercial human breast tissue microarrays (TMA) from normal, benign ductal carcinoma *in situ* (DCIS), invasive and metastatic DCIS were evaluated. The expression of LASP-1 was undetectable in the normal human breast epithelium, but present in myoepithelial cells (Fig. 1A). In the benign DCIS, the expression of LASP-1 was dramatically increased in the cytosol but some tissue cores showed nuclear LASP-1 (6.7%) (Fig.1B). In the case of metastatic DCIS with sheets of cancer cells and no discernible mammary acini, LASP-1 was evident in the nuclei in 42.4% of the cores (Fig. 1C & D).

Expression level of LASP-1 and cell surface CXCR4 in human breast cancer cells

When we evaluated the expression level of LASP-1 and CXCR4 in human breast cancer cell lines, all of the tested luminal and basal-like breast cancer cell lines had robust LASP-1 expression except for BT549. β-tubulin served as the loading control (Fig. 2A). To examine the expression of the cell surface CXCR4 we utilized FACS analysis. In order to assess the specificity of the anti-CXCR4 antibody (12G5 clone), we employed HEK-293 parental cells, HEK-293 cells overexpressing CXCR4 (CXCR4-NS), HEK-293 cells with stable knock down of overexpressed CXCR4 (CXCR4-KD) (83% knock down of CXCR4 –Fig. 2B left panel) so as to verify whether the antibody can track the changes in the level of CXCR4. In HEK-293 parental cells, there was a small amount of CXCR4 expressed (blue trace) compared to the isotype control (purple trace). As expected, CXCR4 overexpressing cells (red trace) revealed a very high expression of CXCR4 which is greatly diminished upon knock down (green trace). The change in MFI values clearly indicated the specificity of the CXCR4 antibody (Fig. 2B right panel). Having verified the specificity of the antibody for CXCR4, we went on to examine the level of cell surface CXCR4 in breast cancer cells using 293-CXCR4 cells as a positive control. (Fig. 2C). MCF7-parental and SKBR3 cell lines had a low expression of cell surface CXCR4 (MFI – 131 and 265 respectively) whereas the MDA-MB-361 cells displayed a moderate level of CXCR4 (MFI - 565). MDA-MB-231S (MDA-MB-231 sorted for high cell surface expression of CXCR4) and MDA-Bone-Un cells (MDA-MB-231 cells re-isolated from mouse bone metastatic lesions) had high levels of cell surface CXCR4 (MFI – 1376 and 1942 respectively).

Chemokines and growth factors induce nuclear translocation of LASP-1

Chemokines and growth factors are abundant in the tumor microenvironment. These can potentially drive the nuclear translocation of LASP-1 in breast cancer and stromal cells. To test this, breast cancer cells expressing CXCR4 and/or EGFR or HER2 were stimulated with CXCL12 or EGF or heregulin. Human microvascular endothelial cells (HMEC) stably expressing CXCR2 (HMEC-CXCR2) were stimulated with a chemokine ligand for CXCR2, CXCL8. Unless stated otherwise, all the breast cancer and the endothelial cells were serum starved and pre-treated with leptomycin B (to block nuclear export) for 2 hours prior to the LASP-1 nuclear translocation assay. Incubation of the MDA-MB-231S cells with 50 nM CXCL12, triggered the nuclear translocation of LASP-1 at 10 min. nLASP-1 was more

pronounced after 30 min and 60 min of stimulation with CXCL12 (Fig. 3A). In contrast, in MDA-Bone-Un cells, even in the absence of exogenous CXCL12 stimulation (50nM), there was marked nuclear accumulation of LASP-1 (Fig. 3B). When SKBR3 cells that express HER2 were stimulated with heregulin (Fig. 3C), there was prominent translocation of LASP-1 to the nucleus at 30 min and extensive nuclear localization at 60 min. MDA-MB-231S cells that were stimulated with EGF showed significant nLASP-1 by 30 and 60 min (Fig. S1A). In order to test whether other chemokine receptors might drive the nuclear shuttling of LASP-1, we evaluated the effect of CXCR2 activation on LASP-1 nuclear translocation in HMEC-CXCR2 cells. At 30 min and 60 min there was a marked accumulation of nLASP-1 (Fig. S1B). The secondary antibody control and the IgG1 isotype control did not contribute any fluorescent background signal (Fig. S1C). We also examined nLASP-1 by biochemical fractionation of cytosolic and nuclear compartments followed by Western blot analysis of LASP-1 (Fig. 3D). In MDA-MB-231S cells that were stimulated with CXCL12, LASP-1 translocated to the nucleus in two peaks, one at 15 min followed by a minor peak at 60 min. In MDA-Bone-Un cells, there was a strong basal accumulation of LASP-1 in the nucleus with additional shuttling of LASP-1 upon treatment of cells with CXCL12 at 15 and 30 min before returning to nearly basal levels at 60 min. In SKBR3 cells stimulated with heregulin, nLASP-1 was induced at 15 min and at 60 min. There was some basal accumulation of LASP-1 observed. When MDA-MB-231S cells were stimulated with EGF, it was hard to observe any induction of nLASP-1 by Western blot analysis. The ligand-induced subcellular distribution profile of LASP-1 in different cell lines (25–150 cells) was quantified and plotted (Fig. S2). These data demonstrate that LASP-1 nuclear translocation occurs in response to several ligands, while basal levels of nLASP-1 vary among cell lines. The reason for the decline in nLASP-1 at different time points is unclear.

Functional assessment of the role of nuclear LASP-1

In order to ascertain the functional role for nLASP-1, LASP-1 was knocked down in MCF7, MDA-MB-231S and MDA-Bone-Un breast cancer cells using previously characterized shRNA constructs ([4]). Stable polyclonal knock down clones were selected with puromycin and the efficiency of knock down of LASP-1 was determined by Western blotting (Fig. 4A). The effect of knock down of LASP-1 in these breast cancer cells was analyzed for effects on 1) ability to form colonies and clusters in 3D-Matrigel, 2) differences in morphological and cytokine secretory profiles 3) changes in the gene expression profile, and 4) the ability to adhere to collagen IV and invade through the Matrigel. The non-silenced (NS) and LASP-1 knock down (LASP-KD) breast cancer cells were cultured on Matrigel and examined for colony growth and morphology. The MCF7-NS cells grew as tumor spheroids, both large and small in size. The MCF7-LASP-KD spheroids were mostly medium sized. In the case of MDA-MB-231S cells, the NS cells grew as a lawn of stellate clusters with extensive arborization whereas the LASP-KD cells grew as isolated stellate clusters with a different morphology (Fig. 4B). Additionally, the effect of silencing of LASP-1 on the secretory profile of chemokines and cytokines in breast cancer cells was examined using a custom-designed antibody microarray targeting chemokines and cytokines in the tumor microenvironment. In MCF7 cells, the level of CCL2 was reduced whereas the levels of CXCL1, 3 and 8 were increased in the media of LASP1-KD cells. The levels of IL-6, GM-CSF and CXCL3 were diminished in MDA-MB-231 parental cells when LASP-1 was

silenced. In MDA-MB-231S cells, the level of GM-CSF was reduced while the level of CXCL8 increased (Fig. S3). Altogether these data suggest that LASP-1 is involved directly or indirectly in cell morphology and cytokine secretion.

Loss of LASP-1 affects the expression profile of genes associated with epithelial to mesenchymal transition (EMT) that influences the adhesive and invasive abilities of the breast cancer cells

To determine whether loss of LASP-1 would result in changes in gene expression, we examined the differential gene expression through oligo microarray analysis in NS and LASP-KD cells (MCF7, MDA-MB-231S and MDA-Bone-Un cells). The quality of the total RNA obtained from the breast cancer cells was analyzed by the integrity of the 28S and 18S rRNAs (Fig. S4). The microarray data has been deposited with the accession number GSE60324 (http://www.ncbi.nlm.nih.gov/geo/query/acc.cgi?acc-GSE60324). We focused here on changes in the mRNA of genes that targets cell adhesion and invasion. Genes encoding cell junction proteins [E-cadherin, claudin, epithelial cell adhesion molecule (EpCAM), **MA**L and **r**elated proteins for **ve**sicle trafficking and membrane **l**ink **d**omain containing-2 (MARVELD2)] and extracellular matrix (ECM) proteins [collagen type IV, secreted protein acidic and rich in cysteine (SPARC) and laminin-α4] and other genes exhibited changes at mRNA level in MCF-7 cells (Table IA). We validated the increase in the protein levels of E-cadherin, α4-integrin, MARVELD2 and EpCAM upon knock down of LASP-1 in MCF7 cells (Fig. 4C). SPARC is known to down regulate E-cadherin in tumor cells ([22]) while p120 catenin is known to stabilize E-cadherin ([23]) ([24]). Thus, the reduction in SPARC and the increase in p120-catenin might explain in part the increase in E-cadherin protein in MCF7 and MDA-MB-361 cell lines (Fig. 4D). In contrast, β-catenin levels did not change. This increase in the level of cell junction proteins and ECM upon knock down of LASP-1 could impair cell motility and invasion.

FAM83B, a protein involved in hyper-activation of the EGF receptor, was up-regulated 6-fold in MCF7 cells with LASP-1 KD. FAM83B is involved in signaling pathways for survival ([25], [26]). It is interesting to note that the transcript for the EGF ligand is also increased 2.3-fold in LASP-1 knock down in MCF7 cells.

In MDA-MB-231S cells, two key microRNAs, miR29B1 and miR29B2, were up regulated upon knock down of LASP-1, which correlated with *reduced transcript levels* for matrix metalloproteinase 9 (MMP9) (Table IB). The miRNA29B is known to down regulate MMP9 mRNA level ([27]). In MDA-Bone-Un cells, cell junction proteins such as claudin12 and cell adhesion molecule2 (CADM2) were up regulated and MMP9 and MMP1 were down regulated upon knock down of LASP-1 (Table IC). Loss of cell adhesion molecule1 (CADM1) is known to induce metastasis of breast cancer and CADM2 may play a similar role ([28]). Collectively, these changes may affect the cell motility and the invasive ability of MDA-MB231S and MDA-Bone-Un cells. The differential effects of LASP-1 silencing on gene expression in luminal versus basal-like breast cancer cells may be due to genetic background differences or differential expression of LASP-2. However, lack of specific antibodies against LASP-2 hinders such investigations. We cannot rule out the possibility that LASP-2 is present in these cells and may compensate for loss of LASP-1.

Based upon the observed changes in expression of adhesion molecules and MMPs accompanying LASP-1 knock down, we went on to evaluate the ability of breast cancer cells to adhere to collagen IV and invade through Matrigel. As expected, MCF7-LASP-KD cells plated onto collagen IV matrix adhered two-fold stronger than the non-silenced control ($p= 0.005$) (Fig. 5A and B). Interestingly, MDA-MB-231-S non-silenced cells seeded onto the Matrigel invaded through the Matrigel 3.5-fold more than the cells that were deficient in LASP-1 ($p<0.0001$) (Fig. 5C and D). Thus LASP-1 appears to modulate the invasiveness of breast cancer cells.

LASP-1 serves as a hub for UHRF1-DNMT1-G9a-Snail1 module

The nuclear protein/protein interactions of LASP-1was also assessed by proteomic analysis of LASP-1 interacting proteins from a triple negative breast cancer cell line (MDA-Bone-Un cells), where LASP-1 knock down (KD) cells were compared to non-silenced cells (NS). This approach allowed us to distinguish proteomic hit coverages in the LASP1-KD cells with that of the NS cells (Table II). We discovered that the association of LASP-1 with the protein known as ‘ubiquitin-like with PHD and ring finger domains 1’ (UHRF1) which was represented by 17 UHRF1 peptides in the for NS cell immunoprecipitate and only 5 peptides in the KD cell immunoprecipitates ($p= 0.003$).

We observed that histone methyltransferase G9a, DNA methyltransferase1 (DNMT1) and histone deacetylase1 (HDAC1) were expressed at a higher level in basal-like breast cancer cells as compared to luminal, while UHRF1 was similar for both basal-like and luminal breast cancer cells (Fig. S5). By employing co-immunoprecipitation and GST-pull down approaches, we validated the association of nLASP-1 with UHRF1,DNMT1, G9a, and the transcription factor Snail1. nLASP-1 was immunoprecipitated from MDA-Bone-Un NS and KD cells and blotted for each of these proteins. nLASP-1 associated more with UHRF1 than DNMT1 upon stimulation with CXCl12 (Fig. 6A). The observed basal association may be due to the presence of LASP-1 in the nucleus (Fig. 3B, 3D and S2,) possibly due to autocrine effects of factors produced by these tumor cells. Interestingly, MDA-Bone-Un cells with LASP-1 knock down (KD) showed equivalent LASP-1 immunoprecipitation compared to the NS cells. Since this cell line showed a high tendency to accumulate LASP-1 in the nucleus even with greater than 70%knock down in the total cell lysate, it appears that there is preferential shuttling of the remaining 30% of LASP1 to the nucleus (Fig. 6E). The LASP1 NS cells displayed a CXCL12-dependent increase in association of LASP-1 to G9 (2.2- fold) and Snail1 (4.4- fold), but just the basal association in KD cells (Fig. 6B).

We postulated that if LASP-1 serves as a hub for epigenetic proteins it may anchor itself to the nuclear actin or bind to methylated histones on one DNA strand before the other strand gets methylated and silenced. We tested this possibility by immunoprecipitating LASP-1 and blotting for associated di- or tri-methylated histone H3 (di-, tri-HH3). LASP-1 associated with di-, tri-HH3 in a CXCL12-dependent manner. There was basal association of LASP-1 with di-, tri-HH3 that increased over 15 min in response to CXCL12, followed by a decline at 30 min (Fig. 6C).

The association of LASP-1 with epigenetic regulatory proteins was further validated by GST-pull down studies. In order to examine the domain/s of LASP-1 that are involved in

mediating the binding of LASP-1 to G9a, UHRF1 and DNMT1, GST-fusion protein constructs of full length LASP-1 and the LIM, LIM-NR and NR-SH3 domains of LASP-1 [that were previously characterized ([4])] were employed (Fig. 6D, left panel). The GST only control did not bind to UHRF1. UHRF1 bound to the full length LASP-1 as a doublet, presumably the phosphorylated and non-phosphorylated forms of UHRF1. The LIM-NR region of LASP-1 showed the stronger association with form of UHRF1 with faster mobility in the gel (Fig. 6D, right panel). LASP-1 may preferentially bind to UHRF1 that appears to be ubiquitinated based on the smeared staining pattern (compared to the lysate lane) and the LIM-NR region of LASP-1 showed the strongest association with UHRF1 (Lower right panel, Fig. 6D). Overall with deductive analysis, the LIM-NR junctional region of LASP-1 appears to mediate the binding to UHRF1, as LIM and NR-SH3 domains have a lower affinity for UHRF1. Both G9a and DNMT1 associated preferentially with the SH3 domain of LASP-1, though G9a bound weakly to the LIM domain of LASP-1 (Fig. 6D).

Next, we tested whether LASP-1 would directly bind to Snail1. Purified GST-Snail1 was mixed with purified recombinant LASP-1, non-bound protein was removed by washing *thrice* with binding buffer, then the LASP-1 directly binding to GST-Snail1 was assessed by Western blotting. Results show LASP-1 indeed directly binds to GST-Snail with negligent binding to GST alone, supporting the concept that LASP-1 can serve as a hub for epigenetic proteins (data not shown).

We then determined whether nLASP-1 would bind to G9a and Snail1 *in situ* in response to the ligand CXCL12. MDA-Bone-Un cells were serum starved and stimulated with CXCL12 for 15 min and the association of nLASP-1 with G9a was assessed by proximity ligation assay (PLA) where co-localization is indicated by the appearance of bright red fluorescent dots. There was a weak basal association of nLASP-1 with G9a, based upon the appearance of red dots of dull intensity. Upon stimulation with CXCL12, the association between nLASP-1 and G9a was stronger as indicated by the brighter dots in the PLA (Fig. 6F). Next, we assessed if nLASP-1 would interact with Snail1 by proximity ligation assay. Upon stimulation with CXCL12, there was increased Snail1 associating with nLASP-1based on the presence of bright red dots (z-stack obtained at the mid nuclear level - Fig. 6G).

Discussion

LASP-1 has been previously shown to translocate to the nucleus in response to forskolin, indicating that $G\alpha_s$-coupled GPCRs can drive the nuclear translocation of LASP-1 ([29]). In this paper, we show that the $G\alpha_i$-coupled chemokine GPCRs, CXCR4 and CXCR2, as well as growth factor receptors EGFR and HER-2 can trigger nuclear shuttling of LASP-1. Increased expression of LASP-1 with increasing malignancy and enhanced nuclear localization of LASP-1 in invasive DCIS clearly suggests a possible role for nLASP-1. Our data show that loss of nLASP-1 resulted in reduced invasiveness, enhanced adhesion, and altered cytokine/chemokine secretion. In advanced cases of breast cancer, nLASP-1 may serve as a hub for UHRF1, DNMT1, G9a and the transcription factor Snail1 as it associates with these epigenetic proteins *as well as with* di, tri-HH3. This has enormous significance as chemokine and growth factor-driven nuclear localization of LASP-1 can potentially alter the proteome through the association of LASP-1 with these key epigenetic proteins. *We*

observed a strong CXCL12-dependent association of nLASP-1 with UHRF1, but only a minor increase with DNMT1. It is possible that other ligands in the tumor microenvironment might influence the association of LASP-1 with DNMT1. Interestingly, UHRF1 confers radio-resistance to breast cancer cells ([30]). G9a epigenetically activates metabolic pathways to sustain cancer cell survival and proliferation ([31, 32]). The interaction of nLASP-1 with G9a in a CXCL12-dependent manner may be significant as knock down of LASP-1 limits proliferation by 40% ([3]). *G9a directly interacts with DNMT1 and forms a complex in the nucleus* ([33]). *The observed association of both G9a and DNMT1 to the SH3 domain of LASP-1 in the GST-pulldown assay may be due to the direct protein-protein interaction between G9a and DNMT.* Up regulation of E-cadherin level when LASP-1 was silenced may be due to two factors: 1) lower mRNA level of SPARC in MCF7 cells coupled with increased p120 catenin; 2) loss of hub activity of nuclear LASP-1 with subsequent destabilization of Snail1. SPARC is known to down regulate E-cadherin level and loss of it may trigger an increase in E-cadherin level.

LASP-1 directly bound to Snail1 in a CXCL12-dependent manner. *We postulate that direct binding of nLASP-1 to Snail1 shields Snail1 from regulatory phosphorylations and degradation that may contribute to metastasis* ([21, 34–39]). Based on these observations, it is possible that CXCL12 and growth factor-mediated nLASP-1 act as a hub in harnessing Snail1 and other EMT master regulators to stabilize their protein level and activity, resulting in regulation of chromatin accessibility and altered gene expression. So through regulation of the stability of Snail1, the gene expression can be fine-tuned to either pro-metastatic or anti-metastatic in nature.

In summary, the novel link described here from CXCL12-CXCR4-LASP1 to the G9a-Snail1 and UHRF1-DNMT1-G9a modules may facilitate breast tumor cell migration, local invasion and metastasis. The reported nuclear role for LASP-1 is a novel component that may be independent of its role in cell migration. The CXCL12-CXCR4-LASP1-Snail1 module might form a novel therapeutic target in the triple negative as well as EGFR and HER2-positive breast cancers. Thus, LASP-1 may serve as a hub for epigenetic activity in the nucleus based on the activation of chemokine GPCRs and growth factor receptors.

Materials and Methods

Cell Culture

i) Human breast cancer cells—Human breast cancer cell lines MCF7, MDA-MB-361, SKBR3, MDA-MB-231 were originally obtained from American Type Culture Collection (ATCC, Manassas, VA) and cultured as described ([13]).

ii) 293-CXCR4 cells—Human embryonic kidney 293 cells (HEK-293, ATCC, Manassas, VA) stably expressing CXCR4 were cultured as described ([4]). These cells will be denoted as 293-CXCR4 cells.

Antibodies

The antibodies were obtained commercially from various sources – 1) Cell Signaling and Technology -Lamin A/C (#4777); EpCAM (#2626S); DNMT1 (#5032P); HDAC1

(#5356P); G9a (3306S); Snail1 (3879P); α4-Integrin (#8440S); β-actin (#4970S); Di, Tri-methyl histone H3 (Lys9) (#5327) 2) Thermoscientific – UHRF1 (PA5-27969) 3) BD Biosciences – E-cadherin (610181); p120-catenin (610133); β-catenin (610154) 4) Bethyl laboratories – MARVELD2 (A301-505A) and 5) Sigma/Aldrich – β-tubulin (T0198).

Analysis of cell surface CXCR4 by fluorescence-activated cell sorting (FACS)

The cell surface expression of CXCR4 on human breast cancer cells was determined as described ([13]).

Three-dimensional (3D) cell culture in Matrigel

50 μL of liquid Matrigel (growth factor-reduced and phenol red-free) (BD Biosciences, Bedford, MA) was laid onto chambered slides. MCF7 or MDA-MB-231 (parental or CXCR4-sorted) cells (3000-5000 cells) were overlaid in 400 μL of media and cultured for 48–72 h.

Antibody microarray

The antibody microarray (RayBiotech Inc., Norcross, GA) was custom-built with several cytokines related to breast cancer progression and metastasis. The microarray membrane was incubated with 1 ml of serum-free media harvested from 3D-cultures MCF-7, MDA-MB-231 parental and MDA-MB-231 sorted for CXCR4 (MDA-231S cells). The blot was processed and developed as per manufacturer's protocol.

Biochemical fractionation

Nuclear and cytosolic fractions were separated by using the 'Nuclei EZ prep' kit (Sigma, St. Louis, MO). Lamin A/C and tubulin were employed to identify the purity of the fractions. In some experiments, the CXCR4 antagonist AMD-3100 (10 μM) (Tocris, Ellisville, MO) was employed to block CXCR4-mediated nuclear import of LASP-1 for 1 h at 37°C.

Stable knock down of LASP-1

LASP-1 was stably knocked down in human breast cancer cells using shRNA. Lentiviruses were generated in 293-FT cells by transfecting the shRNA constructs for LASP-1 (V2LHS_64685 and V2LHS_64686; Open Biosystems, Huntsville, AL) and a non-silencing construct (NS-control). Briefly, 3 μg of the shRNA mir plasmid, 2 μg of psPAX2 and 1 μg of pMD2.G were transfected into 293-FT cells. Media were collected at 48 h and 72 h, pooled and concentrated. After the viral transduction, cells were selected with puromycin and the level of LASP-1 knock down was determined by Western blot analysis.

Stable knock down of CXCR4

CXCR4 was stably knocked down in HEK-293 cells using shRNA construct for CXCR4 (TRCN0000256864 validated clone; Sigma, St. Louis, MO). Briefly, 6 μg of the shRNA mir plasmid was transfected into HEK-293 cells, selected with puromycin and CXCR4 knock down was determined by Western blot analysis using anti-CXCR4 antibody (2B11 clone) (BD Biosciences, San Jose, CA).

Tissue microarray studies

De-identified human normal breast and breast cancer tissue microarrays (Cybrdi and US Biomax, Rockville, MD) were subjected to deparaffinization, dehydration and rehydration followed by antigen retrieval by heating the slides at 95°C in Citrate buffer, pH 6.0 for 10 min. The cores were blocked with 'Background Sniper' (Biocare Medical, Concord, CA) and LASP-1 was visualized with mouse monoclonal anti-LASP1 antibody (1:50) (Covance, Princeton, NJ) followed by Donkey anti-mouse Cy3 secondary antibody (1:100) (Jackson Immunoresearch, West Grove, PA) or Goat anti-mouse AlexaFluor594 (Life Technologies, Grand Island, NY). The nuclei were stained with Hoechst (Life Technologies, Grand Island, NY). The immunoreactivity against LASP-1 was scanned at the Digital Histology Core at Vanderbilt University and also evaluated by confocal microscopy.

DNA Oligo microarray analysis

Total RNA was isolated from human breast cancer cells (Non-silenced and LASP-1 KD cells) cultured on 3D-Matrigel using the RNA-STAT 60 kit (Amsbio, Lake Forest, CA). The quality of the total RNA was tested at the Vanderbilt VANTAGE core and the RNA integrity number (RIN value) ranged from 9.6–10 (high quality). Total RNA with high RIN values and 28S:18S ratio was subjected to microarray analysis. The changes in gene expression upon knock down of LASP-1were analyzed with Affymetrix human Gene 1.0 ST and 2.0 ST arrays (Affymetrix, Santa Clara, CA). The microarray experiments were performed in 2–4 biological replicates. The results were analyzed by PARTEK Genomics software.

Mass spectrometric identification of LASP-1 interacting proteins

One-dimensional and Multidimensional protein identification technology (MudPIT) was employed to identify novel proteins that interact with LASP-1 in 'Bone-Un' cells. Monoclonal anti-LASP1 antibody (MMS-426P, Covance, Princeton, NJ) was cross-linked to Protein G magnetic beads (EMD Millipore, Billerica, MA) with Bis(sulfosuccinimidyl)suberate (BS^3) (Sigma/Aldrich, St. Louis, MO) following the manufacturer's protocol. BS^3 is a homo-bifunctional, non-cleavable cross-linker. The 'Bone-Un' cells (Non-silenced and LASP1-KD) were lysed in co-immunoprecipitation buffer pH (Co-IP buffer) 8.0 (50 mM Tris, pH 8.0, 150 mM NaCl, 1% IGEPAL-40, 0.5% sodium deoxycholate, and 5 mM EDTA) with proteinase inhibitor cocktail I and phosphatase inhibitor cocktails 2 and 3 (Sigma/Aldrich, St. Louis, MO). LASP-1 and its associated proteins were immunoprecipitated from cell lysates (1 mg) and nutated for 2 h at 4°C. The immune complexes were washed twice with the Co-IP buffer and once with Tris-buffered saline, pH 7.5 to remove unbound proteins. Bound proteins were eluted and analyzed at the proteomics core at Vanderbilt University. The results were annotated using Scaffold 4.0 software (Proteome Software, Inc., Portland, OR).

Proximity ligation assay

The proximity ligation assay (PLA) allows detection of any two interacting proteins *in vivo* or *in situ* using antibodies raised in two different species. A pair of oligonucleotide-labeled secondary antibodies (PLA probes) will generate a signal only when the two PLA probes are in close proximity. The signal from each detected pair of PLA probes will be visualized as a

distinct fluorescent spot. Duolink *In Situ* Orange Fluorescent kit (Sigma/Aldrich, St. Louis, MO) was employed to detect the interaction between 1) LASP-1 and G9a and 2) LASP-1 and Snail. The PLA was performed according to manufacturer's instructions. The images were acquired by confocal microscopy.

Co-immunoprecipitation of LASP-1 with LASP-1 interacting proteins

Human breast cancer cells were serum-starved and incubated with Leptomycin B for 2 h and stimulated with CXCL12. Pure nuclei were isolated (Nuclei EZ prep kit, Sigma, St. Louis, MO) and the nuclear proteins were extracted with a buffer (50 mM Tris, pH 8.0, 350 mM NaCl, 1 mM DTT, protease and phosphatase inhibitors, 5 mM $MgCl_2$ and 50 units of DNAse I) for 1 h at 4°C. LASP-1 was immunoprecipitated from the clarified nuclear lysate and analyzed for any associated proteins as described ([4]).

Cell adhesion assay

Control-silenced and LASP1-knock down MCF7 cells were trypsinized and recovered for 2 h in DMEM / 10%FBS. A 96-well plate pre-coated in triplicate with collagen IV (200 μg/mL) (Sigma/Aldrich, St. Louis, MO) and blocked with the binding buffer (DMEM with 0.1% BSA) both for 1 h at 37°C were loaded with cells (8000) and allowed to adhere to the coated surface for 1 h at 37°C. The wells were washed and the adhered cells were fixed with 4% paraformaldehyde, permeabilized with 1% Triton-X-100 and the nuclei were visualized with DAPI. The fluorescent nuclei were counted from five randomly selected fields and the experiment was repeated thrice.

Matrigel invasion assay

Matrigel invasion assay was performed (according to the manufacturer's protocol (BD Biosciences, San Jose, CA). The cells on the top surface were scraped off and the invaded cells that adhered onto the bottom side of the membrane were then fixed, stained with 0.1% crystal violet and counted from five randomly selected fields and the experiment was repeated thrice.

Image J analysis

The band intensities of proteins were quantified by using Image J analysis 1.47v.

Statistical analysis

The data from the cell adhesion and Matrigel invasion assays were analyzed by unpaired 't' test with Welch's correction using the Prism software version 5.0 (GraphPad, La Jolla, CA). The average and the standard error mean (S.E.M.) were calculated and the 'p' value is presented in the data. For both cell adhesion and Matrigel invasion assays, five randomly selected fields were counted and the experiment was repeated thrice (3 biological replicates).

Supplementary Material

Refer to Web version on PubMed Central for supplementary material.

Acknowledgments

This work was supported by Department of Defense, IDEA grant W81XWH-11-1-0413 (D.R.), VICTR award– supported in part by Vanderbilt Clinical and Translational Science Award (CTSA) grant – UL1 TR000445 from NCRR/NIH (D.R.), NIH grants CA-34590 (to A.R.), VA Merit Award (to A. R.), Career Scientist Award (to A.R.) from the Tennessee Valley Healthcare System and the Department of Veterans Affairs, and Ingram Professorship (to A.R.).

References

1. Orth MF, Cazes A, Butt E, Grunewald TG. An update on the LIM and SH3 domain protein 1 (LASP1): a versatile structural, signaling, and biomarker protein. Oncotarget. 2015 Jan 1; 6(1):26–42. [PubMed: 25622104]
2. Lin YH, Park ZY, Lin D, Brahmbhatt AA, Rio MC, Yates JR 3rd, et al. Regulation of cell migration and survival by focal adhesion targeting of Lasp-1. J Cell Biol. 2004 May 10; 165(3):421–32. [PubMed: 15138294]
3. Grunewald TG, Kammerer U, Schulze E, Schindler D, Honig A, Zimmer M, et al. Silencing of LASP-1 influences zyxin localization, inhibits proliferation and reduces migration in breast cancer cells. Exp Cell Res. 2006 Apr 15; 312(7):974–82. [PubMed: 16430883]
4. Raman D, Sai J, Neel NF, Chew CS, Richmond A. LIM and SH3 protein-1 modulates CXCR2-mediated cell migration. PloS one. 2010; 5(4):e10050. [PubMed: 20419088]
5. Raman D, Neel NF, Sai J, Mernaugh RL, Ham AL, Richmond A. Characterization of chemokine receptor interacting proteins using a proteomics approach to define the CXCR2 “chemosynapse”. Meth Enzymol. 2009; 460:297–312.
6. Neel, NF. PhD Dissertation. Vanderbilt University; 2008. Regulation of CXC chemokine receptor function through intracellular trafficking and novel receptor-interacting proteins.
7. Strieter RM, Burdick MD, Mestas J, Gomperts B, Keane MP, Belperio JA. Cancer CXC chemokine networks and tumour angiogenesis. Eur J Cancer. 2006 Apr; 42(6):768–78. [PubMed: 16510280]
8. Addison CL, Daniel TO, Burdick MD, Liu H, Ehlert JE, Xue YY, et al. The CXC chemokine receptor 2, CXCR2, is the putative receptor for ELR+ CXC chemokine-induced angiogenic activity. J Immunol. 2000 Nov 1; 165(9):5269–77. [PubMed: 11046061]
9. Yang L, Huang J, Ren X, Gorska AE, Chytil A, Aakre M, et al. Abrogation of TGF beta signaling in mammary carcinomas recruits Gr-1+CD11b+ myeloid cells that promote metastasis. Cancer Cell. 2008 Jan; 13(1):23–35. [PubMed: 18167337]
10. Muller A, Homey B, Soto H, Ge N, Catron D, Buchanan ME, et al. Involvement of chemokine receptors in breast cancer metastasis. Nature. 2001 Mar 1; 410(6824):50–6. [PubMed: 11242036]
11. Smith MC, Luker KE, Garbow JR, Prior JL, Jackson E, Piwnica-Worms D, et al. CXCR4 regulates growth of both primary and metastatic breast cancer. Cancer Res. 2004 Dec 1; 64(23):8604–12. [PubMed: 15574767]
12. Luker KE, Luker GD. Functions of CXCL12 and CXCR4 in breast cancer. Cancer Lett. 2006 Jul 8; 238(1):30–41. [PubMed: 16046252]
13. Ueda Y, Neel NF, Schutyser E, Raman D, Richmond A. Deletion of the COOH-terminal domain of CXC chemokine receptor 4 leads to the down-regulation of cell-to-cell contact, enhanced motility and proliferation in breast carcinoma cells. Cancer Res. 2006 Jun 1; 66(11):5665–75. [PubMed: 16740704]
14. Li H, Yang L, Fu H, Yan J, Wang Y, Guo H, et al. Association between Galphai2 and ELMO1/Dock180 connects chemokine signalling with Rac activation and metastasis. Nat Commun. 2013; 4:1706. [PubMed: 23591873]
15. Fulton AM. The chemokine receptors CXCR4 and CXCR3 in cancer. Curr Oncol Rep. 2009 Mar; 11(2):125–31. [PubMed: 19216844]
16. Goldberg-Bittman L, Neumark E, Sagi-Assif O, Azenshtein E, Meshel T, Witz IP, et al. The expression of the chemokine receptor CXCR3 and its ligand, CXCL10, in human breast adenocarcinoma cell lines. Immunol Lett. 2004 Mar 29; 92(1–2):171–8. [PubMed: 15081542]

17. Walser TC, Rifat S, Ma X, Kundu N, Ward C, Goloubeva O, et al. Antagonism of CXCR3 inhibits lung metastasis in a murine model of metastatic breast cancer. Cancer Res. 2006 Aug 1; 66(15): 7701–7. [PubMed: 16885372]

18. Grunewald TG, Kammerer U, Kapp M, Eck M, Dietl J, Butt E, et al. Nuclear localization and cytosolic overexpression of LASP-1 correlates with tumor size and nodal-positivity of human breast carcinoma. BMC cancer. 2007; 7:198. [PubMed: 17956604]

19. Frietsch JJ, Grunewald TG, Jasper S, Kammerer U, Herterich S, Kapp M, et al. Nuclear localisation of LASP-1 correlates with poor long-term survival in female breast cancer. Br J Cancer. 2010 May 25; 102(11):1645–53. [PubMed: 20461080]

20. Stefansson OA, Esteller M. Epigenetic modifications in breast cancer and their role in personalized medicine. Am J Pathol. 2013 Oct; 183(4):1052–63. [PubMed: 23899662]

21. Zheng H, Kang Y. Multilayer control of the EMT master regulators. Oncogene. 2014 Apr 3; 33(14):1755–63. [PubMed: 23604123]

22. Robert G, Gaggioli C, Bailet O, Chavey C, Abbe P, Aberdam E, et al. SPARC represses E-cadherin and induces mesenchymal transition during melanoma development. Cancer research. 2006 Aug 1; 66(15):7516–23. [PubMed: 16885349]

23. Ireton RC, Davis MA, van Hengel J, Mariner DJ, Barnes K, Thoreson MA, et al. A novel role for p120 catenin in E-cadherin function. The Journal of cell biology. 2002 Nov 11; 159(3):465–76. [PubMed: 12427869]

24. Davis MA, Ireton RC, Reynolds AB. A core function for p120-catenin in cadherin turnover. The Journal of cell biology. 2003 Nov 10; 163(3):525–34. [PubMed: 14610055]

25. Cipriano R, Bryson BL, Miskimen KL, Bartel CA, Hernandez-Sanchez W, Bruntz RC, et al. Hyperactivation of EGFR and downstream effector phospholipase D1 by oncogenic FAM83B. Oncogene. 2014 Jun 19; 33(25):3298–306. [PubMed: 23912460]

26. Cipriano R, Miskimen KL, Bryson BL, Foy CR, Bartel CA, Jackson MW. FAM83B-mediated activation of PI3K/AKT and MAPK signaling cooperates to promote epithelial cell transformation and resistance to targeted therapies. Oncotarget. 2013 May; 4(5):729–38. [PubMed: 23676467]

27. Chou J, Lin JH, Brenot A, Kim JW, Provot S, Werb Z. GATA3 suppresses metastasis and modulates the tumour microenvironment by regulating microRNA-29b expression. Nature cell biology. 2013 Feb; 15(2):201–13. [PubMed: 23354167]

28. Wikman H, Westphal L, Schmid F, Pollari S, Kropidlowski J, Sielaff-Frimpong B, et al. Loss of CADM1 expression is associated with poor prognosis and brain metastasis in breast cancer patients. Oncotarget. 2014 May 30; 5(10):3076–87. [PubMed: 24833255]

29. Mihlan S, Reiss C, Thalheimer P, Herterich S, Gaetzner S, Kremerskothen J, et al. Nuclear import of LASP-1 is regulated by phosphorylation and dynamic protein-protein interactions. Oncogene. 2012 Jun 4. Eng.

30. Li X, Meng Q, Rosen EM, Fan S. UHRF1 confers radioresistance to human breast cancer cells. Int J Radiat Biol. 2011 Mar; 87(3):263–73. [PubMed: 21067293]

31. Dong C, Wu Y, Yao J, Wang Y, Yu Y, Rychahou PG, et al. G9a interacts with Snail and is critical for Snail-mediated E-cadherin repression in human breast cancer. J Clin Invest. 2012 Apr 2; 122(4):1469–86. [PubMed: 22406531]

32. Dong C, Yuan T, Wu Y, Wang Y, Fan TW, Miriyala S, et al. Loss of FBP1 by Snail-mediated repression provides metabolic advantages in basal-like breast cancer. Cancer cell. 2013 Mar 18; 23(3):316–31. [PubMed: 23453623]

33. Esteve PO, Chin HG, Smallwood A, Feehery GR, Gangisetty O, Karpf AR, et al. Direct interaction between DNMT1 and G9a coordinates DNA and histone methylation during replication. Genes & development. 2006 Nov 15; 20(22):3089–103. [PubMed: 17085482]

34. Peinado H, Ballestar E, Esteller M, Cano A. Snail mediates E-cadherin repression by the recruitment of the Sin3A/histone deacetylase 1 (HDAC1)/HDAC2 complex. Mol Cell Biol. 2004 Jan; 24(1):306–19. [PubMed: 14673164]

35. Olmeda D, Jorda M, Peinado H, Fabra A, Cano A. Snail silencing effectively suppresses tumour growth and invasiveness. Oncogene. 2007 Mar 22; 26(13):1862–74. [PubMed: 17043660]

36. Olmeda D, Moreno-Bueno G, Flores JM, Fabra A, Portillo F, Cano A. SNAI1 is required for tumor growth and lymph node metastasis of human breast carcinoma MDA-MB-231 cells. Cancer Res. 2007 Dec 15; 67(24):11721–31. [PubMed: 18089802]

37. Peinado H, Olmeda D, Cano A. Snail, Zeb and bHLH factors in tumour progression: an alliance against the epithelial phenotype? Nat Rev Cancer. 2007 Jun; 7(6):415–28. [PubMed: 17508028]

38. Batlle E, Sancho E, Franci C, Dominguez D, Monfar M, Baulida J, et al. The transcription factor snail is a repressor of E-cadherin gene expression in epithelial tumour cells. Nat Cell Biol. 2000 Feb; 2(2):84–9. [PubMed: 10655587]

39. Thiery JP, Sleeman JP. Complex networks orchestrate epithelial-mesenchymal transitions. Nat Rev Mol Cell Biol. 2006 Feb; 7(2):131–42. [PubMed: 16493418]

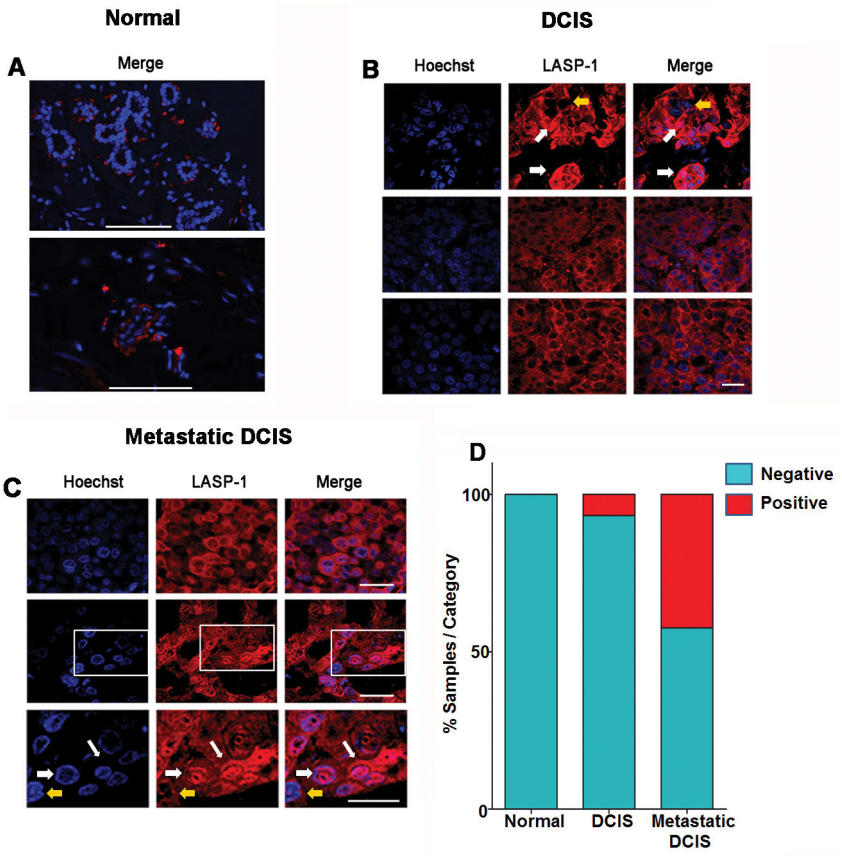

Fig. 1. Localization of LASP-1 in normal human breast and malignant breast epithelial cells *in vivo*

A) *Confocal images of normal human breast tissue cores* – Normal human breast tissue microarray cores were processed for immunohistochemistry (n=69, with two representative cores shown). Merged images are shown in which LASP-1 was pseudo-colored red and the nuclei blue. Images represent single z-stack section of 0.5 μm.

B) *Confocal images of DCIS and invasive DCIS breast cancer cores*– Human ductal carcinoma in situ (DCIS cores (Invasive ductal carcinoma – n=68; Ductal carcinoma – n=20) were processed for immunohistochemistry (three representative patient cores are shown). LASP-1 and the nuclei were pseudo-colored red and blue respectively. Images represent single z-stack section of 0.5 μm. White arrows point to nuclear LASP-1 and yellow arrows point to the absence of LASP-1 in the nucleus.

C) *Confocal image of breast cancer tissue cores from metastatic DCIS*– Metastatic DCIS cores were processed for immunohistochemistry. (n=32; two different patients shown). LASP-1 and the nuclei were pseudo-colored red and blue respectively. Boxed areas in the middle row were enlarged and shown below. Images represent single z-stack section of 0.5 μm. White arrows point to nuclear LASP-1 and yellow arrows point to the absence of LASP-1 in the nucleus.

D) *Quantification of nuclear positivity and negativity for LASP-1 in normal and cancerous breast cores*– The tissue cores were analyzed for the presence or absence of LASP-1 in the nucleus of normal and cancerous breast epithelial cells. The % distribution of LASP-1 was plotted and shown.

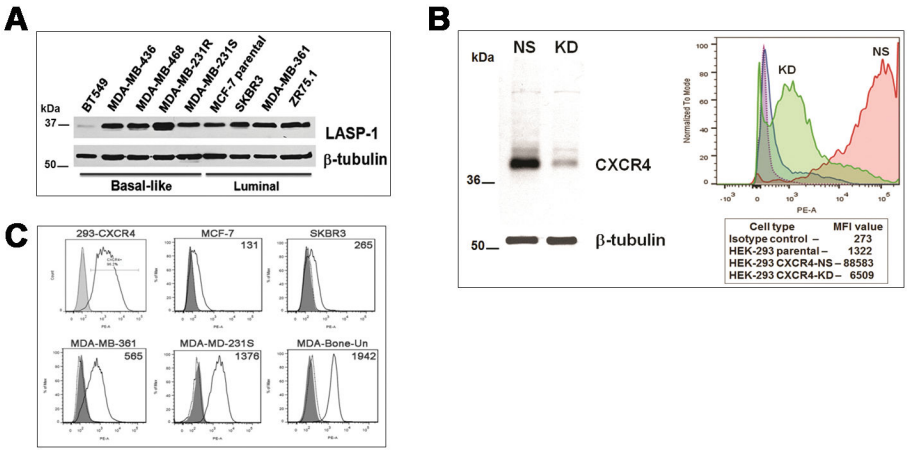

Fig. 2. Expression level of LASP-1 and cell surface CXCR4 in a panel of breast cancer cell lines

A) *Expression level of LASP-1*– 30 μg of total lysate from luminal and basal-like breast cancer cell lines were separated by 10% SDS-PAGE and blotted for LASP-1. MDA-MB-231R – parental MDA-MB-231 cells; MDA-MB-231S – MDA-MB-231 cells FACS sorted for high cell surface CXCR4; β-tubulin served as the loading control.

B) *CXCR4 antibody is specific for CXCR4* – Human embryonic kidney cells (HEK-293 - denoted as parental), HEK-293 cells overexpressing human CXCR4 (NS), HEK-293 cells with stable knock down of overexpressed CXCR4 were analyzed for cell surface CXCR4 with mouse monoclonal anti-CXCR4 (mAB170 - 12G5 clone) by FACS analysis. The shaded and the dotted peaks represent the gating and isotype controls, respectively, and solid peaks represent CXCR4. 293-CXCR4 cells served as a positive control. The mean fluorescent index (MFI) indicates the level of cell surface CXCR4. Dotted purple peak – IgG2A isotype control; Blue peak – Low endogenous level of CXCR4; Red peak – Overexpressed CXCR4; Green peak – Stably knocked down CXCR4.

C) Cell surface expression level of CXCR4 is higher in the basal-like than luminal breast cancer cell lines – Cell surface CXCR4 was probed with mouse monoclonal anti-CXCR4 (mAB170 - 12G5 clone) and analyzed by FACS analysis. The mean fluorescent index (MFI) indicates the level of cell surface CXCR4. The representative FACS scan was shown and the experiment was repeated thrice.

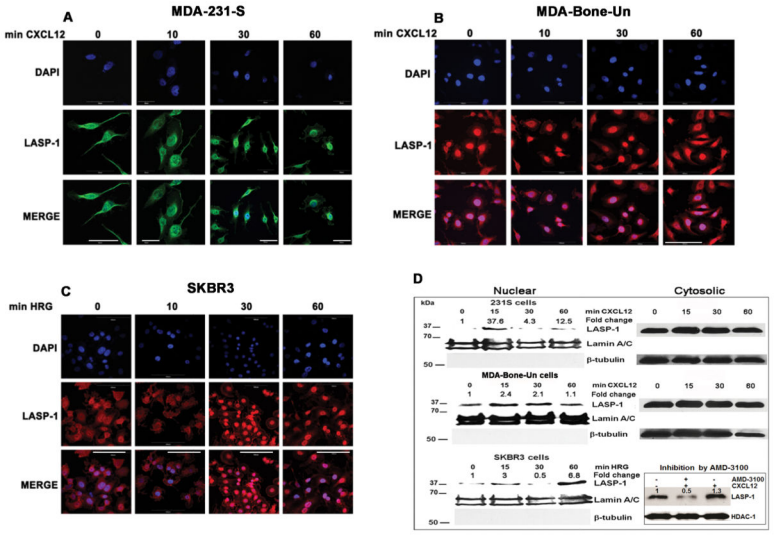

Fig. 3. LASP-1 translocates to the nucleus of breast cancer cells in response to chemokines and growth factors

A) MDA-MB-231S breast cancer cells were serum starved and stimulated with 50 nM CXCL12 for the indicated time points. LASP-1 and the nuclei were pseudo-colored red and blue respectively. Images represent single z-stack section of 0.5 μm. Scale bar – 50 μm for all except for 10 min time point set at 30 μm.

B) MDA-Bone-Un breast cancer cells were serum starved and stimulated with 50 nM CXCL12 for the indicated time points. LASP-1 and the nuclei were pseudo-colored red and blue respectively. Images represent single z-stack section of 0.5 μm. Scale bar – 100 μm.

C) SKBR3 breast cancer cells were serum starved and stimulated with 50 ng / mL Heregulin for the indicated time points. LASP-1 and the nuclei were pseudo-colored red and blue, respectively. Images represent single z-stack section of 0.5 μm. Scale bar – 100 μm.

D) MDA-MB-231S, SKBR3 and MDA-Bone-Un breast cancer cells were stimulated with CXCL12 or Heregulin for the indicated time points. The nuclear and the cytosolic fractions were separated and analyzed for nuclear translocated LASP-1. Lamin A/C and β-tubulin were used to identify the purity of the nuclear and cytosolic fractions. Right bottom panel – MDA-Bone-Un breast cancer cells were stimulated with CXCL12 with and without the CXCR4 antagonist AMD-3100. The nuclear lysates were analyzed for the imported LASP-1 level by Western blotting. Histone deacetylase1 (HDAC1) served as the loading control. The experiment was repeated twice.

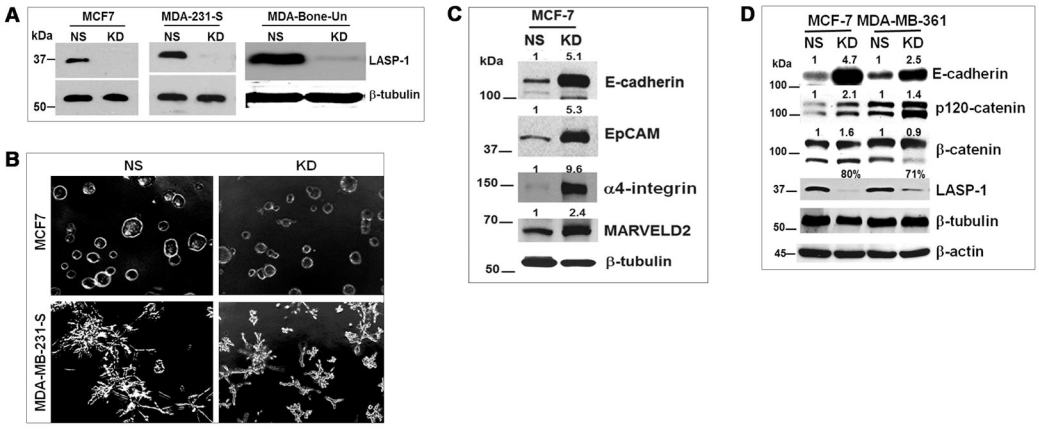

Fig. 4. Stable silencing of LASP-1 in breast cancer cells alters cell growth and expression of proteins favor cell-cell adhesion under 3D conditions

A) *Stable knock down of LASP-1.* LASP-1 was stably knocked down by employing short hairpin microRNAs through lentiviral mediated transduction into different breast cancer cells. The knock down efficiency was followed by Western blotting of total cell lysates for LASP-1. β-tubulin served as the loading control.

B) MCF7 and MDA-231S cells that were stably silenced for LASP-1 expression were cultured in Matrigel and their growth under 3D conditions was assessed. The micrographs were obtained at 200X magnification.

C) *Up regulated expression of several cell adhesion genes upon knock down of LASP-1.* 20 μg of total cell lysates from non-silenced (NS) and LASP-1 knock down MCF7 cells were separated by SDS-PAGE and blotted for E-cadherin, EpCAM, α4-integrin and MARVELD2. β-tubulin and β-actin served as the loading controls. The band intensities of proteins were quantified by using Image J analysis and normalized to β-actin. The fold change was given above the bands.

D) *Up regulated* e*xpression of E-cadherin and p120-catenin occurs upon knock down of LASP-1 in luminal breast cancer cell lines*: 20 μg of total cell lysates from non-silenced (NS) and LASP-1 knock down MCF7 and MDA-MB-361 cells were separated by SDS-PAGE and blotted for E-cadherin, p120-catenin and β-catenin. The % of knock down for LASP-1 is given above the LASP-1 bands. The fold change is given above the E-cadherin, p120-catenin and β-catenin bands. The experiment was repeated twice and the representative blot is shown. β-tubulin and β-actin served as the loading controls.

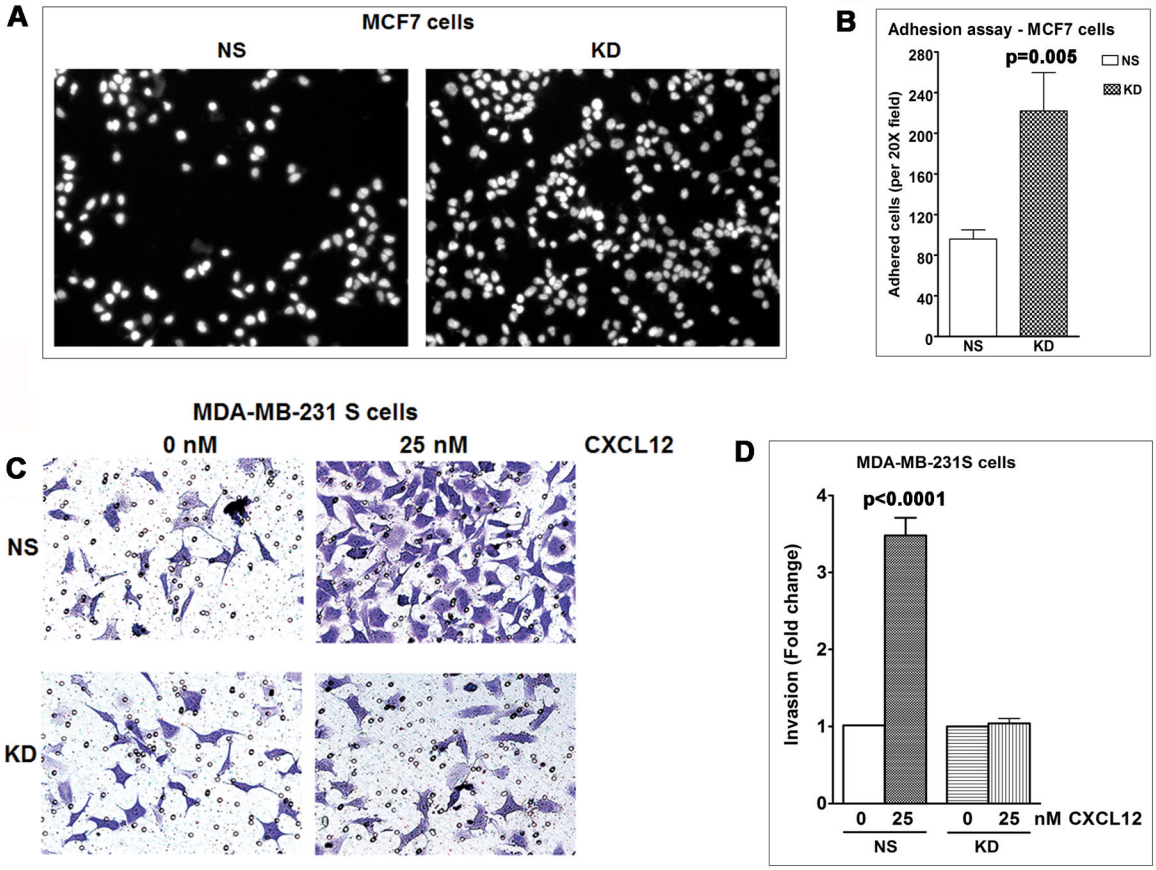

Fig. 5. Functional analysis of LASP-1 on adhesion and Matrigel invasion properties of breast cancer cells

A) and B) *LASP-1 knock down increases adhesion to collagen IV matrix.*

MCF7 breast cancer cells (8000 cells) were allowed to adhere to collagen IV matrix. The adhered cells were stained with DAPI and counted from 5 randomly selected fields. The data from 3 independent experiments were plotted with standard error mean (S.E.M.) ($p=0.005$ – for 25nM CXCL12 concentration).

C) and D) *LASP-1 knock down impairs optimal invasive ability of breast cancer cells through Matrigel.*

MDA-231-S breast cancer cells (1×10^5 cells) were seeded onto the Matrigel and were allowed to migrate to the bottom side of the partition membrane with bottom wells containing 25 nM CXCL12 overnight. The migrated cells were fixed, stained with 0.1% Crystal violet, and counted from 5 randomly selected fields. The data from 3 independent experiments were plotted with standard error mean (S.E.M.) ($p<0.0001$).

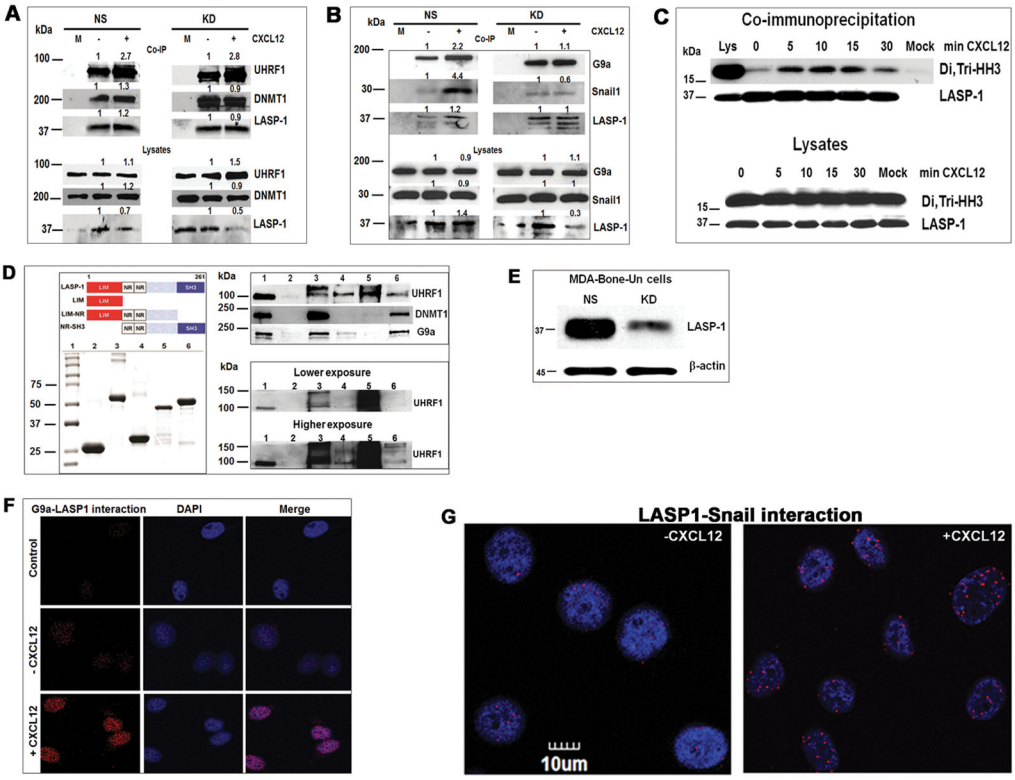

Fig. 6. LASP-1 associates with epigenetic proteins UHRF1, DNMT1, G9a and Snail1

A) *LASP-1 co-immunoprecipitates with UHRF1 and DNMT1.* 100 μg of the nuclear extracts from MDA-Bone-Un cells stimulated with vehicle (0 min) or 500 ng /ml of CXCL12 for 15 min were incubated with control mouse monoclonal IgG (Mock) or with mouse anti-LASP-1 antibody. LASP1-bound proteins were eluted and analyzed for endogenous LASP-1 and associated proteins UHRF1 and DNMT1. Bottom panel: 15 μg of total cell lysates from MDA-Bone-Un cells that were stimulated with vehicle (0 min) or CXCL12 for 15 min. LASP-1 lysate blot was obtained after stripping and re-probing for LASP-1 after the detection of Snail1 first. The experiment was repeated twice and the representative blot was quantified and shown. NS – Non-silenced control; KD – LASP-1 knock down. The band intensities of proteins were quantified by using Image J analysis and normalized to their respective non-stimulated control (bands in -CXCL12 lane). The fold change was given above the bands to track the level of the immunoprecipitated proteins with respect to their protein levels in the lysates.

B) *LASP-1 co-immunoprecipitates with G9a and Snail1.* 100 μg of the nuclear extracts from MDA-Bone-Un cells stimulated with vehicle (0 min and Mock) or 500 ng /ml of CXCL12 for 15 min were incubated with control mouse monoclonal IgG (Mock) or with mouse anti-LASP-1 antibody. Bound proteins were eluted and analyzed for endogenous LASP-1 and associated G9a and Snail1. NS – Non-silenced control; KD – LASP-1 knock down. Bottom panel: 15 μg of total cell lysates from MDA-Bone-Un cells that were stimulated with vehicle (0 min) or CXCL12 for 15 min. LASP-1 lysate blot was obtained after stripping and re-probing for LASP-1 after the detection of Snail1 first. The experiment was repeated twice and the representative blot was quantified and shown. NS – Non-silenced control; KD –

LASP-1 knock down. The band intensities of proteins were quantified by using Image J analysis and normalized to their respective non-stimulated control (bands in -CXCL12 lane). The fold-change was given above the bands to track the level of the immunoprecipitated proteins with respect to their protein levels in the lysates.

C) *LASP-1 co-immunoprecipitates with Di-, Tri-methylated histone H3*. Total cell lysates from MDA-Bone-Un cells stimulated with vehicle (0 min) or 200 ng /ml of CXCL12 for 5, 10, 15 and 30 min were incubated with control mouse monoclonal IgG (Mock) or with mouse anti-LASP-1 antibody. The proteins were eluted and analyzed for endogenous LASP-1 and associated di-, tri-methylated histone H3. Bottom panel: 15 μg of total cell lysates from MDA-Bone-Un cells that were stimulated with vehicle (0 min) or CXCL12 for 5, 10, 15 and 30 min were blotted for LASP-1 and di-, tri-methylated histone H3. The experiment was repeated thrice and the representative blot was shown.

D) *LASP-1 associates with UHRF1, DNMT1 and G9a in the GST pull down assay.*

Left panel: *Purification of GST, full length and different domains of LASP-1fused to GST.* 20 μg purified GST and GST-LASP1 (full length) and different domains of LASP-1 fused to GST were separated by 10% SDS-PAGE and stained by colloidal Coomassie blue. Lane1 – M.W. markers; Lane 2 – GST; Lane 3 – GST-LASP1; Lane 4 – GST-LIM; Lane 5 – GST-LIM-NR; Lane 6 – GST-NR-SH3.

Right top panel: *LASP-1 associates with UHRF1, DNMT1 and G9a in the GST pull down assay*. 200 μg purified GST and GST-LASP1 proteins were mixed with 1–1.5 mg of total lysate from MDA-Bone-Un cells. Bound proteins were eluted and analyzed for association of LASP-1 with endogenous UHRF1, DNMT1 and G9a. The experiment was repeated thrice and the representative blot was shown. Lane 1 – 15 μg of lysate; Lane 2 – GST; Lane 3 – GST-LASP1; Lane 4 – GST-LIM; Lane 5 – GST-LIM-NR; Lane 6 – GST-NR-SH3.

Right bottom panel: *LASP-1 appears to associate with ubiquitinated UHRF1*. In some GST-pull down experiments, associated UHRF1 appeared smeared but distinct; a lower and a higher exposure of the same blot were shown. Lane 1 – 15 μg of lysate; Lane 2 – GST; Lane 3 – GST-LASP1; Lane 4 – GST-LIM; Lane 5 – GST-LIM-NR; Lane 6 – GST-NR-SH3.

E) Stable knockdown of LASP-1. MDA-Bone-Un cells employed in the co-immunoprecipitation (Co-IP) experiments were re-analyzed again to know the level of stable knock down of LASP-1 at the time of Co-IP experiment by Western blotting of total cell lysates (30 μg) for LASP-1. β-actin served as the loading control.

F) and G) *LASP-1 associates with G9a and Snail1 in situ in a CXCL12-dependent manner.* MDA-Bone-Un breast cancer cells that were grown on glass coverslips were stimulated with and without CXCL12 for 15 min. The cells were fixed and subjected to proximity ligation assay. The experiment was repeated twice and the representative images are shown.

Table I

Stable silencing of LASP-1 alters the gene expression profile differentially in luminal and basal-like breast cancer cells.

IA. Stable silencing of LASP-1 alters the gene expression profile when MCF7 breast cancer cells are cultured in 3D.

MCF7 breast cancer cells that were grown on Matrigel were lysed, total RNA was isolated and analyzed for changes in gene expression upon knock down of LASP-1 (n=4; biological replicates).

IB. Stable silencing of LASP-1 alters the gene expression profile when MDA-MB-231S breast cancer cells are cultured in 3D.

MDA-MB-231S breast cancer cells that were grown on Matrigel were lysed, total RNA was isolated and analyzed for changes in gene expression upon knock down of LASP-1 (n=2; biological replicates).

IC. Stable silencing of LASP-1 alters the gene expression profile when MDA-Bone-Un breast cancer cells are cultured in 3D.

MDA-Bone-Un breast cancer cells that were grown on Matrigel were lysed, total RNA was isolated and analyzed for changes in gene expression upon knock down of LASP-1 (n=2; biological replicates).

Table IA. Changes in gene expression governing cell adhesion and other key genes upon knock down of LASP-1 in MCF7 cells.			
Gene name	**Fold Change**	**Accession #**	**‘q’ value (‘p’ value - KD vs. NS)**
Family with sequence similarity 111, member B (FAM111B)	17.0	NM_198947	0.00014
MARVEL domain containing 2 (MARVELD2)	14.8	NM_001038603	0.00014
Epithelial cell adhesion molecule (EpCAM)	13.9	NM_002354	0.00014
3-oxoacid CoA transferase 1	12.6	NM_000436	0.00015
Leucine-rich repeat-containing G protein-coupled receptor 5 (LGR5)	9.6	NM_003667	0.0009
Scinderin	6.8	NM_001112706	0.00038
Glycerol-3-phosphate dehydrogenase 2 (GPD2)	6.1	NM_001083112	0.00014
Claudin1	5.9	NM_021101	0.003
Secreted frizzled-related protein2 (SFRP2)	5.9	NM_003013	0.0004
MAPK13	4.6	NM_002754	0.0002
Hyaluronan Synthase 2	4.5	NM_005328	0.001
Thrombospondin 4 (THBS4)	4.5	NM_003248	0.00015
Histone cluster 2, H2BF	4.1	NM_001024599	0.0002
Integrin α4 (ITGA4)	3.7	NM_000885	0.00014
Collagen and calcium binding EGF domains 1 (CCBE1)	3.3	NM_133459	0.00023
Laminin α4 (LAMA4)	2.9	NM_001105206	0.00014
Rab9A	2.9	NM_004251	0.00029
Aldehyde dehydrogenase 1 family, member A2 (ALDH1A2)	2.7	NM_003888	0.0008
Collagen, typeXIV α1 (Col14A1)	2.7	NM_021110	0.00015
E-cadherin (CDH1)	2.3	NM_004360	0.00052
Hemicentin	2.3	NM_031935	0.0003
Sox5	2.3	NM_152989	0.003
Deubiquitinase USP9X	2.3	NM_001039590	0.0008

Table IA. Changes in gene expression governing cell adhesion and other key genes upon knock down of LASP-1 in MCF7 cells.

Gene name	Fold Change	Accession #	'q' value ('p' value - KD vs. NS)
Cancer/testis antigen family 45, member A6	−17.0	NM_001017438	0.00024
Cancer/testis antigen family 45, member A1	−14.4	NM_001017417	0.00076
Cancer/testis antigen family 45, member A2	−13.2	NM_152582	0.00044
Cancer/testis antigen family 45, member A5	−12.2	NM_001007551	0.00039
Cancer/testis antigen family 45, member A4	−12.0	NM_001017436	0.001
Cancer/testis antigen family 45, member A3	−11.5	NM_001017435	0.0009
Tenomodulin	−10.3	NM_022144.2	0.00025
Calcitonin-related polypeptide β	−5.0	NM_000728	0.0005
LIM and SH3 protein1 (LASP-1)	−3.3	NM_006148	0.00025
Fucosyltransferase 9	−2.6	NM_006581	0.0014
Secreted protein, acidic, cysteine- rich (SPARC) / Osteonectin	−2.6	NM_003118	0.002
Fibrillin1	−2.3	NM_000138	0.00044
Aldolase C, fructose-bisphosphate	−2.3	NM_005165	0.0009

Table IB. Changes in key genes in upon knock down of LASP-1 in MDA-MB-231S cells.

Gene name	Fold Change	Accession #
Chemokine (C-C motif) ligand 7 (CCL7)	2.5	NM_006273
MicroRNA 29B1 (miR29B1)	2.4	NR_029517
Interferon, α7 (IFNA7)	2.4	NM_021057
Glycine receptor, α3 (GLRA3)	2.4	NM_006529
Family with sequence similarity 48, member B1 (FAM48B1)	2.1	NM_198947
Apolipoprotein L1 (APOL1)	2.1	NM_003661
Keratin associated protein 9-3 (KRTAP9-3)	2.1	NM_031962
MicroRNA 29B2 (miR29B2)	2.0	NR_029518
Hyaluronan Synthase 2	2.0	NM_005328
Lectin, galactoside-binding, soluble, 13 (LGALS13)	2.0	NM_013268
Interferon, α17 (IFNA17)	1.9	NM_021268
Frizzled homolog 3 (FZD3)	1.9	NM_017412
Protocadherin β15 (PCDHB15)	1.8	NM_018935
Tetratricopeptide repeat domain 30A (TTC30A)	1.8	NM_152275
miRLet7F1	2.3	NR_029483
LIM and SH3 protein1 (LASP- 1)	−5.2	NM_006148
MicroRNA 320E (miR320E)	−2.8	NR_036157
Nuclear RNA export factor 5 (NXF5)	−2.6	NR_028089
Secreted phosphoprotein 1 (SPP1)	−2.5	NM_001040058
Gamma-glutamyltransferase 1 (GGT1)	−2.1	NM_005265
Matrix metalloproteinase 9 (MMP9)	−2.0	NM_004994
Leucine rich repeat containing 32 (LRRC32)	−1.9	NM_005512
S100A11	−1.8	NM_005620

Table IC. Changes in gene expression upon knock down of LASP-1 in MDA-Bone-Un cells.		
Gene name	**Fold Change**	**Accession #**
Family with sequence similarity 75, member D4 (FAM75D4)	3.3	NM_001145197
Claudin12	2.9	ENST00000416322
MicroRNA 519A1 (miR519A1)	2.9	NR_030218
Calpain 3, (p94) (CAPN3)	2.6	NR_027911
MicroRNA 506 (miR506)	2.4	NR_030233
Major histocompatibility complex, class II, DR β1 (HLA-DRB1)	2.3	NM_002124
Fibronectin leucine rich transmembrane protein 3 (FLRT3)	2.0	NM_198391
MANSC domain containing 1 (MANSC1)	2.0	NM_018050
Fibronectin leucine rich transmembrane protein 3 (FLRT3)	2.0	NM_198391
Keratin 37	1.9	NM_003770
Histone cluster 1, H4b	1.9	NM_003544
Cell adhesion molecule 2 (CADM2)	1.8	NM_001167674
MicroRNA 1224 (miR1224)	1.8	NR_030410
LIM and SH3 protein1 (LASP-1)	−4.8	NM_006148
SSX1	−2.5	NM_005635
Sec16B	−2.3	ENST00000354921
Leucine rich repeat containing 18 (LRRC18)	−1.9	NM_001006939
Matrix metalloproteinase 9 (MMP9)	−1.9	NM_004994
Matrix metalloproteinase 1 (MMP1)	−1.8	NM_002421
Dual specificity phosphatase and pro-isomerase domain containing 1 (DUPD1)	−1.8	NM_001003892

Table II

Association of novel proteins with LASP-1 – Number of peptides analyzed by 1D run and MudPIT proteomic analysis.
Identification of novel proteins that bind to LASP-1 by proteomic analysis.
LASP-1 was immunoprecipitated from non-silencing and LASP-1 knock down MDA-Bone-Un breast cancer cells and the eluted proteins were analyzed by 1D run and MudPIT analysis (n=3; biological replicates).

Protein	1D Run- NS	1D Run - KD	MudPIT - NS	MudPIT- KD	Fisher's Exact Test (p value)
LASP-1	13	1	32	7	0.0001
Phosphoglycerate kinase	15	6	27	16	0.0001
Ezrin	5	1	-	-	-
Spectrin α-chain, non-erythrocytic 1	-	-	28	13	-
Nucleolin	11	6	-	-	-
E3 Ubiquitin ligase, UHRF1	-	-	17	5	0.0034
N-acetyltransferase 10	-	-	12	7	0.063
Protein disulfide isomerase A5	-	-	12	3	0.02
Apoptosis inhibitor 5	-	-	10	5	-
Cytokeratin 18	-	-	15	2	0.0044
Keratin 2a	9	1	-	-	-
Ras-GAP BP2	-	-	10	4	-
AP3 complex, Subunit μ1	-	-	10	3	-
Nuclear receptor co- repressor 2	-	-	11	3	-
Cell division kinase 12 (Cdk12)	-	-	11	3	
Unconventional myosin-1c	-	-	14	7	0.031
Actin-related protein 3 (Arp3)	-	-	12	6	0.04
Clathrin heavy chain 1	12	4	-	-	-